Eur. Phys. J. C (2024) 84:1207
https://doi.org/10.1140/epjc/s10052-024-13579-8

THE EUROPEAN PHYSICAL JOURNAL C

Regular Article

Experimental Physics

Ionization loss spectra of high-energy protons in an oriented crystal at various incidence angles with respect to a crystalline plane

S. V. Trofymenko[1,2,a], **I. V. Kyryllin**[1,2,b]

[1] Akhiezer Institute for Theoretical Physics, National Science Center "Kharkiv Institute of Physics and Technology", Akademichna Str., 1, 61108 Kharkiv, Ukraine
[2] V.N. Karazin Kharkiv National University, Svobody Sq. 4, 61022 Kharkiv, Ukraine

Received: 1 August 2024 / Accepted: 5 November 2024

Abstract The ionization energy loss distributions (spectra) of high-energy protons in oriented silicon crystals are considered on the basis of computer simulation. Evolution of the spectra with the change of the angle θ between the particle momentum and the crystal (110) plane is investigated. It is shown that both the most probable and the average energy loss change non-monotonically with the increase of θ. While at small θ these losses are lower than their values in a disoriented crystal, at larger θ they can be higher than these values. The dependence of the most probable energy loss on θ contains a discontinuity, which however might be challenging to register experimentally. Additionally, the influence of dechanneling and the incident beam divergence on the spectra of planar channeled protons is demonstrated.

1 Introduction

Penetration of a high-energy charged particle through a medium is accompanied by different processes of the particle energy loss. They include several types of electromagnetic radiation (bremsstrahlung, Cherenkov, transition, channeling etc.) and energy loss on excitation and ionization of atoms known as ionization energy loss (or simply, ionization loss). Incident hadrons are likely to trigger nuclear reactions as well. In thin silicon detectors the ionization loss leads to production of electron–hole pairs, which create a measurable current upon application of an external voltage. Thereby, it is possible to measure the ionization loss of each separate particle of the beam and investigate the probability distribution of the value of this loss in the case when the beam current is not very high. In thin amorphous targets, or disoriented crystalline detectors, this probability distribution, which we will further call the ionization loss spectrum (ILS),[1] was derived by Landau [1] and further investigated both theoretically [2–6] and experimentally [7–9]. In [10,11] the evolution of ILS with the change of the target thickness has been investigated with the use of disoriented silicon detectors of smoothly tunable thickness of the depleted layer. In [12–15] the ILS of electron-positron pairs under the condition of the Chudakov effect in very thin detectors has been investigated.

In [16–19] the ILS of high-energy particles in oriented crystals has been experimentally studied. The peculiarity of this case is in the fact that when a charged particle enters a crystal at a small angle with respect to a crystalline axis or plane, the channeling mode of motion can take place [20]. In this mode the particle is trapped in a potential well created either by separate atomic planes or strings (in the case of negatively charged particles) or by neighboring planes or strings (for positively charged particles). Particularly, positively charged particles, being repelled from the planes and strings, experience a reduced amount of close collisions with atoms losing less energy. As shown in [16–19], this leads to a shift of the ILS maximum, corresponding to the most probable value of the particle ionization energy loss in the target, to the region of smaller losses (see Fig. 1). In [21] a method of measuring the dechanneling length of negatively charged particles on the basis of their ILS registration was proposed. In [22] a way of implementation of this method with the use of oriented silicon detectors of smoothly tunable thickness has been discussed.

[a] e-mail: strofymenko@gmail.com (corresponding author)
[b] e-mail: i.kyryllin@gmail.com

[1] It is sometimes referred to as straggling function.

Published online: 22 November 2024

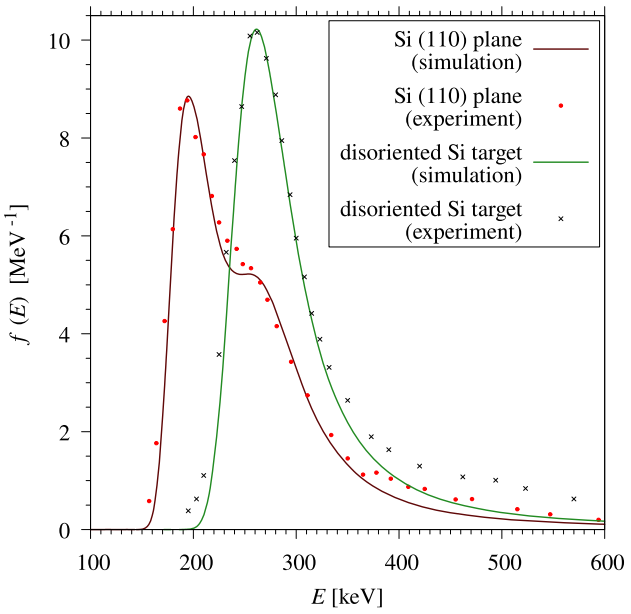

Fig. 1 Ionization loss spectra of 15 GeV/c protons in a silicon target of 900 μm thickness. Dots and crosses – experimental results from [18], solid lines – simulation

In the cited works, only the case when the mean direction of the incident particle beam is parallel to the crystal axes or planes, along with the particle penetration through a disoriented crystal, has been considered. However, these investigations indicate that in oriented crystals ILS is rather sensitive to the particle mode of motion. Thus, studying ILS at various crystal orientations with respect to the incident particle beam may provide a valuable information on the properties of particle motion in oriented crystals and on the change of these properties with the change of the crystal orientation. In the present work, on the basis of a newly elaborated method of simulation of high-energy particle ionization loss in oriented crystals we investigate evolution of ILS with the change of the angle between the incident particle momentum and the crystal plane. It is shown that in this case the shape of the spectra can noticeably differ from the one typical for amorphous targets and the value of the most probable energy loss E_{MP} changes non-monotonically, reflecting peculiarities of the particle motion at different incidence angles. As an example, we consider the motion of 15 GeV/c protons in a silicon crystal of 900 μm thickness. This choice is motivated by existence of a set of experimental measurements of ILS for such a proton momentum and crystal thickness, for the case when the major atomic planes of the crystal were successively oriented along the mean direction of the proton beam [18], which allows to test the simulation method comparing the results with the experiment in this particular case.

2 On the simulation method

For simulation of a particle ionization loss we separate it into contributions of distant and close collisions. Simulation of the distant collision contribution is based on the expression for the probability of exciting or ionizing the atom by the incident particle as a fucntion of the particle impact parameter ρ. For the atom excited from the ground state $|1\rangle$ to a state $|k\rangle$, which may belong to either discrete or continuous spectrum, and an ultrarelativistic incident particle this probability can be presented as follows (see, e.g. [23]):

$$w_k(\rho) = 4\alpha^2 |\xi_{k1}|^2 \Omega_{k1}^2 K_1^2(\Omega_{k1}\rho), \tag{1}$$

where

$$\Omega_{k1}^2 = \left(\omega_{k1}^2/\gamma^2 + \omega_p^2\right)/c^2, \tag{2}$$

K_1 is the Macdonald function, $\hbar\omega_{k1}$ is the energy difference of the states, $\xi_{k1} = \langle k|\xi|1\rangle$ is the matrix element of the atomic electron coordinate for the considered transition (e.g., $\xi = x$, y or z), $\gamma \gg 1$ is the incident particle Lorentz-factor, $\alpha \approx 1/137$ – is the fine-structure constant, ω_p is the plasma frequency of the medium. On the basis of this expression it is possible to derive the effective cross section of the particle energy transfer to an atomic electron, which depends on the particle coordinates in the transversal plane (the one perpendicular to the crystalline plane or axis along which the particle moves). This cross section is applied for simulating the value of the particle energy loss due to distant collisions on each small interval of its trajectory. The particle trajectory is defined by numerical solution of the equation of its motion in the averaged potential of atomic stings or planes, depending on the crystal orientation. The particle incoherent scatterings on atomic electrons and thermal vibrations of atoms are taken into account. For details of the particle motion simulation procedure see [24–27].

Energy transfers due to close collisions are simulated with the use of Rutherford cross section of free-particle scattering. Presently we neglect deviations from this cross section at energy transfers of the order of the maximum energy which can be transferred in a single collision, associated with the specific type of the incident particle. This is possible since such huge energy transfers do not contribute to ILS in the vicinity of its maximum (the region we are mainly interested in), which is shaped by softer collisions.

In order to test validity of the applied method, a comparison of the simulated ILS with some available experimental results [18] for 15 GeV/c protons moving in an oriented and disoriented silicon crystal of 900 μm thickness has been performed. The results of this comparison are shown in Fig. 1.

For the oriented crystal, the comparison is made for the case when the crystal (110) atomic planes are oriented along the mean direction of the proton momentum in the incident beam. The beam divergence of one crytical angle of planar channeling (which we estimate as $\theta_c \approx 53.4$ μrad), reported in [18], is taken into account. The ILS of protons in such conditions is shown in Fig. 1 by the brown curve. The corresponding experimental data is shown by the red dots. Possible additional error introduced into the experimental results by the procedure of their digitalisation on the basis of the figures presented in [18], is estimated as being up to 7 keV on the horizontal axis and up to 0.12 MeV^{-1} on the vertical one. The green curve in the figure represents the ILS for the case of the disoreinted Si crystal. It has a shape of a conventional Landau distribution, typical for amorphous targets, which is slightly modified by the effects of the atomic electron binding. The corresponding experimental data is shown by the black crosses. In both cases (oriented and disoriented Si crystal) the experimental distributions were normalized to fit the hights of the simulated spectra at their maxima (in [18] the absolute spectra hights were not presented). The figure indicates that the developed method of the ionization loss simulation provides ILS rather nicely coinciding with the experimentally measured spectra, which allows applying this method to the study of orientational effects for ILS. Some discrepancies in the high-energy tails of the distributions might be attributed to some background inevitable in the experiment, which may originate, e.g., from the thermal noise in the detector. We are inclined to attribute this discrepancy to the background since additional comparison of our simulation results with the results of systematic experimental investigations of ILS in disoriented silicon crystals under the condition of a negligibly small noise [8] demonstrated rather nice coincidence not only in the vicinity of the ILS maximum, but also in the region of its high-energy tail.

3 Dependence of ILS on the angle between the particle momentum and the atomic plane (110) of the crystal

In [28] it was shown that the probability of close collisions (PCC) of a high-energy positively charged particle with the atoms of a crystal significantly depends on the angle θ between the particle momentum and the atomic plane along which the particle is moving. As this angle increases from zero to the critical angle of planar channeling θ_c, the PCC rises sharply, reaching a maximum at $\theta = \theta_c$, and then begins to decrease, leveling off to a constant at θ around several values of θ_c. As noted in [28], the presence of this maximum is associated with the phenomenon of 'hanging' of positively charged particles over atomic planes, when they spend more time close to the atoms of the plane. The characteristic parameter which determines the particle motion mode in this case is its orthogonal energy

$$\varepsilon_\perp = \frac{pv\theta^2}{2} + U(x),$$

where p and v are the particle momentum and velocity, the x axis is orthogonal to the atomic planes, and $U(x)$ is the potential of the atomic planes. Here we use the continuous potential model of atomic planes proposed by Lindhard [20] and consider this potential as averaged over thermal vibrations of the atoms. The value of $U(x)$ at x corresponding to the positions of the atomic planes is taken to equal zero. The x coordinates of the atomic planes are denoted below as x_i. At angles $\theta < \theta_c$, the particle orthogonal energy is negative. In this case the particle motion in the direction of x axis in the potential well formed by two adjacent planes is finite. 'Hanging' over atomic planes takes place at $\theta \approx \theta_c$. The angle θ_c is determined by the condition $pv\theta_c^2/2 = -U_0$, where $U_0 < 0$ is the minimum value of $U(x)$ in the region between the planes. At $\theta \approx \theta_c$, when the particle x coordinate is close to x_i, the particle is decelerated in the direction of x axis, which results in an increased PCC. For $\theta > \theta_c$, the particle motion in the direction of x axis is above-barrier and the larger the angle θ, the less the particle is decelerated along the x axis crossing the atomic planes. Due to this fact, it is natural to expect a significant dependence of the ILS shape on the angle θ, since this spectrum is formed by energy losses due to both distant and close collisions. Below, in order to investigate a 'pure' manifestation of this orientational dependence for ILS, we neglect the incident beam divergence.

Let us first analyze the influence of incoherent scattering of particles during planar channeling on the shape of their ILS. Figure 2 shows the ILS of 10^6 protons with the momentum of 15 GeV/c moving in a silicon crystal of 900 μm thickness in the field of (110) atomic planes (solid curve), entering the crystal parallel to these planes, and in a disoriented silicon target of the same thickness (dot-dashed curve). We see that the value of E_{MP}, corresponding to the maximum of the spectrum, in the case of planar orientation of the crystal is approximately one and a half times less than in the case of the disoriented silicon target. It is explained by the fact that during planar channeling, positively charged particles move in a potential well formed by neighboring atomic planes. The center of this well is located midway between adjacent atomic planes, so most of the particles, while moving in the crystal in the mode of planar channeling, do not come close to the atoms of the crystal, which means that the PCC for them is less than in the case of motion in a disoriented crystal. Therefore, on average, they lose less energy than in the disoriented crystal.

Figure 2 shows that while the ILS of protons in the disoriented crystal is a Landau distribution, the ILS corresponding

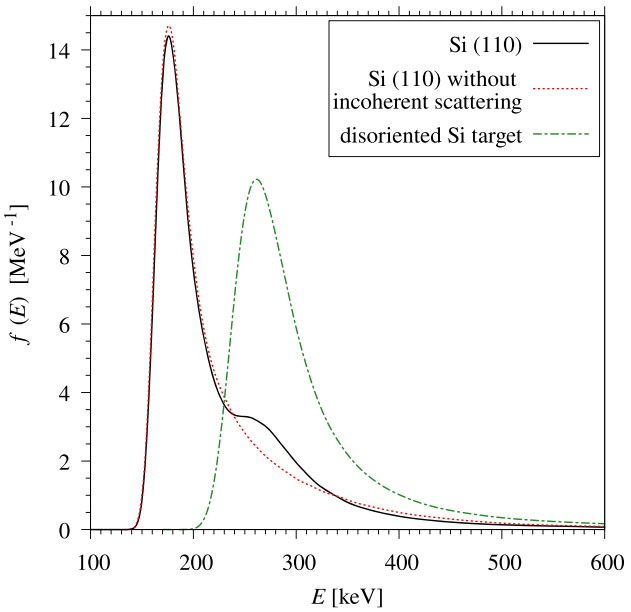

Fig. 2 ILS of 15 GeV/c protons during planar channeling in the field of (110) planes of a silicon crystal with (solid line) and without (dotted line) incoherent scattering, as well as during motion in the disoriented crystal (dash-dotted line)

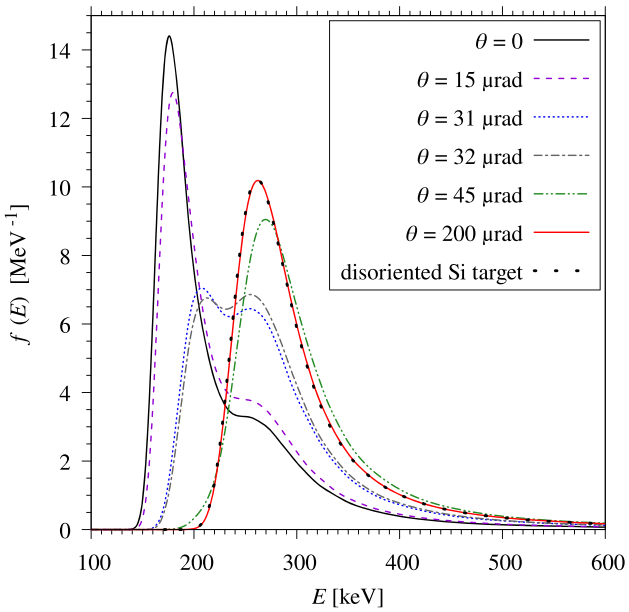

Fig. 3 ILS of 15 GeV/c protons at various angles between the particle momentum and the (110) plane of the silicon crystal

to planar channeling has, in addition to the main peak, a hump at the energy loss of $E \approx 270$ keV. The presence of this hump is associated with a small group of particles which due to incoherent scattering in the crystal become above-barrier, i. e. dechannel. For above-barrier particles, the value of E_{MP} is close to its value in the disoriented crystal. In order to prove that the mentioned hump is explained by dechanneling, we also present the ILS of protons in a planar-oriented crystal without taking into account incoherent scattering on thermal vibrations of atoms and electronic subsystem of the crystal by the dotted curve in Fig. 2. Without incoherent scattering, there is no dechanneling. As we see, in this case there is no hump in the ILS, which is similar to the Landau distribution.

Note that comparing Figs. 1 and 2, it is also possible to see the impact of the beam divergence angle of one θ_c on the ILS of the proton beam in the planar-oriented crystal, since the presented here simulation results differ just by taking into account (Fig. 1) and not taking into account (Fig. 2) such a divergence. As we see, on the one hand, this divergence results in the increase of the hump due to dechanneled particles. On the other hand, it leads to the shift of ILS maximum position and change of the value of E_{MP} by about 20 keV. The decrease of the maximum hight in Fig. 2 is caused by the increase of the hump, since the surface under the curve $f(E)$ should remain fixed due to normalization condition $\int f(E)dE = 1$.

Now, let us consider evolution of the ILS of protons with the momentum of 15 GeV/c with the change of the angle θ between the direction of the particle incidence and the (110) plane of the silicon crystal. Figure 3 shows the ILS for different values of the angle θ. For each θ the passage of 10^6 protons through the crystal was simulated. In Fig. 3, we see that as the angle θ increases, the value of E_{MP} of the protons increases, which is explained by both the increase in the number of above-barrier particles and the increase of the PCC of protons due to their 'hanging' over atomic planes. The first process leads to the increase of the hump in the distribution, while the second one – to the shift of the distribution maximum to the right. The increase in the number of above-barrier particles leads to a decrease of the height of the peak corresponding to channeled particles in the ILS, and an increase of the height of the peak corresponding to above-barrier particles. At a certain angle, this leads to the situation when the peak formed by channeled particles becomes lower than the peak formed by above-barrier ones. In the Figure, this occurs between $\theta = 31$ μrad and $\theta = 32$ μrad. When the angle θ becomes much greater than θ_c, the distribution becomes similar to the ILS of protons in a disoriented crystal. Let us note that at $\theta \approx \theta_c$ the ILS is slightly shifted towards larger energy loss compared to the ILS of protons in a disoriented crystal. This shift is associated with the increased PCC of 'hanging' particles at $\theta \approx \theta_c$, discussed at the beginning of this section.

Let us now consider the dependence of the proton most probable ionization energy loss E_{MP} on the angle θ in more detail. This dependence is shown in Fig. 4. It is based on the simulation of passage of 10^6 protons through a silicon crystal at different values of the angle θ which was changed in steps of 2 μrad. As θ increases from 0 to about θ_c, we

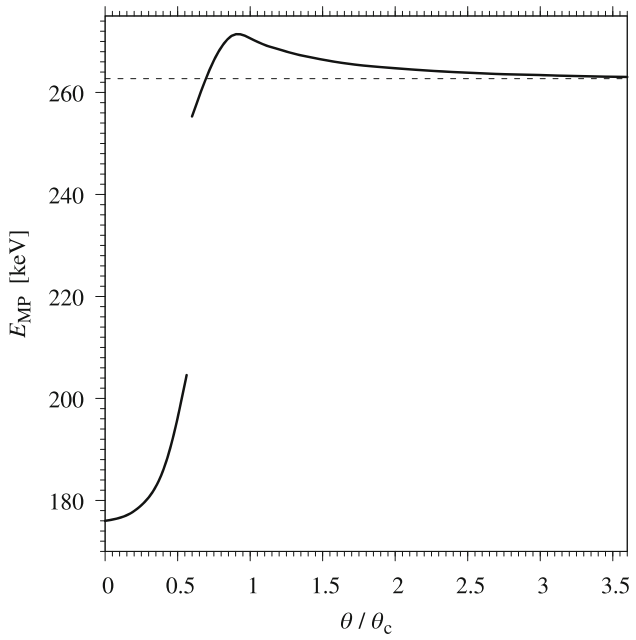

Fig. 4 Solid line – dependence of the most probable energy loss of protons E_{MP} on the angle θ, dashed line – the value of E_{MP} for the disoriented crystal

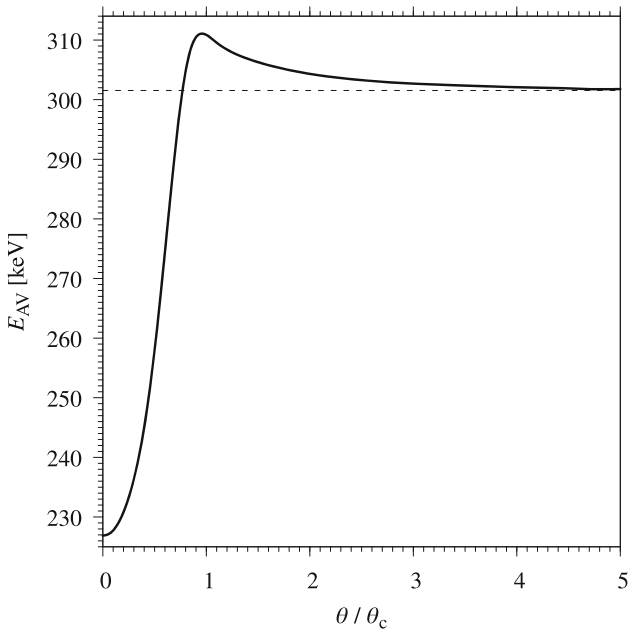

Fig. 5 Solid line – dependence of the average restricted energy loss of protons E_{AV} on the angle θ, dashed line – the value of E_{AV} for the disoriented crystal

see a monotonous increase of E_{MP}. Notably, at $\theta \approx \theta_c$, the value of E_{MP} exceeds E_{MP} in the disoriented crystal, which is shown in Fig. 4 by the dashed line. As the angle θ further increases, E_{MP} begins to decrease and eventually approaches the value of E_{MP} in the disoriented crystal when $\theta \gg \theta_c$. The discontinuity in the line $E_{MP}(\theta)$ in Fig. 4 corresponds to the angle at which the peak in ILS, associated with above-barrier particles, becomes higher than the peak associated with channeled particles. It results in the 'jump' of E_{MP} from the value corresponding to the second peak to the value corresponding to the first one. Though, as we see, on the left and on the right side of the discontituity the function $E_{MP}(\theta)$ has rather close values of the derivatives. This makes experimental observation of this discontituity challenging, since it may rather look like a very steep increase of a continuous function.

Along with E_{MP}, another important quantity, which can be defined from experimental measurements of ILS, is the average restricted value of the particle ionization energy loss in the target E_{AV}. Presently, we will define this quantity as

$$E_{AV} = \int_0^{E_0} f(E) E dE, \tag{3}$$

where E_0 is some value of the particle ionization loss in the target which is chosen as an upper restriction of the integration region in (3). The point is that, in order to calculate the quantity (3) from the experimentally measured spectrum, it is necessary to subtract the background contribution to $f(E)$. It is a feasible task in the region $E \sim E_{MP}$, where the number of counts in the detector is rather high, but may lead to a poor precision of the obtained results in the region of large E in the tail of the distribution, where the relative contribution of the background is much higher (see, e.g. Fig. 1). In this case, it is practical to choose the value E_0 in (3) as a one, at which the relative contribution of the background to $f(E)$ is still rather low.

Figure 5 shows the dependence of E_{AV} on the angle θ between the direction of the proton momentum and the (110) plane of the silicon crystal. Presently, we choose E_0 to equal 600 keV, i. e. the energy at which the range of delta electrons incide the target becomes of the order of the target thickness.[2] We see that in the present case E_{AV} varies in a similar way as E_{MP}, though it does not have a discontinuity, typical for the latter. Also, comparing Figs. 4 and 5, we see that in the considered case the quantity E_{MP} is somewhat more sensitive to the crystal orientation than E_{AV}. Namely, the range of E_{MP} variation (the difference between its maximum and minimum value) is around 36% of the value of this quantity in a disoriented crystal, while for E_{AV} this range reaches about 28% of the value marked by the dashed line in Fig. 5. This slight difference in sensitivity of E_{MP} and E_{AV} to the crystal orientation may be attributed to the following circum-

[2] At higher energies, delta electrons leave the target (detector) without disposing of all their energy inside it, and the particle energy loss due to knocking out such electrons cannot be properly registered. Though, such a restriction, relied on the energy transfer in a single collision, is more natural for the quantity defined by the expression (4) (see the discussion after this formula) and is presently applied just as an example.

stance. Increasing the angle θ up to the maxima of $E_{\rm MP}(\theta)$ and $E_{\rm AV}(\theta)$ dependences, we increase the number of incident proton collisions with atoms, which results in the increase of the ionization loss. To some extent, such an increase in the number of collisions is analogous to the increase of the target thickness L without the change of its orientation. It is known that the quantity $E_{\rm MP}$ increases faster with the thickness than $E_{\rm AV}$. Particularly, in amorphous targets $E_{\rm AV} \propto L$ while $E_{\rm MP} \propto L(\ln L + A)$, where A is some constant.

Let us note that the quantity defined by the expression (3) is generally not identical to the conventional value of the average restricted ionization loss which for a unit path of the proton in an amorphous target is [29][3]

$$\frac{dE}{dx} = \frac{2\pi n Z e^4}{mv^2}\left[\ln\frac{2mv^2\gamma^2 E_1}{I^2} - \beta^2 - \delta(\gamma)\right]. \tag{4}$$

Here v and γ are the proton velocity and Lorentz-factor, m is the electron mass, n and Z are the atomic density and atomic number of the medium, I is its mean ionization potential, $\beta = v/c$, δ is the density effect correction. The difference between (3) and (4) is associated with the fact that in (4) E_1 has a physical sence of energy transferred by the proton to an atomic electron in a single collision, which is chosen from some considerations to restrict the interval of integration with respect to transferred energies. In (3) the 'restricting' energy E_0 has a physical sence of the proton energy loss in the target, which can be a sum of energy losses in several or more collisions. In each of them the transferred energy is less than E_0. Thus, the value of (3) corresponds to the value of (4) at some $E_1 < E_0$. In the case when the same restriction $E_1 = E_0$ is chosen in both expressions, the formula (3) is expected to lead to a smaller value than (4). With the increase of E_0, the quantities (3) and (4) tend to become identical, provided $E_1 = E_0 \ll E_{\rm max}$.

To illustrate the above, let us calculate the quantity (4) for 15 GeV/c protons in a disoriented silicon target of 900 μm thickness, taking $E_1 = 600$ keV, which is the same value as the one chosen for E_0 in Fig. 5. Presently, $E_1 \ll E_{\rm max}$ since $E_{\rm max} \approx 2mv^2\gamma^2 \approx 260$ MeV. The density effect correction can be estimated as follows [30]:

$$\delta(\gamma) = 4.606\left[X - X_a + (X_a - X_0)\left(\frac{X_1 - X}{X_1 - X_0}\right)^r\right], \tag{5}$$

where for silicon $X_0 = 0.2$, $X_1 = r = 3$. Also

$$X_a = 0.217\left(2\ln\frac{I}{\hbar\omega_p} + 1\right), \qquad X = \log_{10}\frac{p}{Mc}, \tag{6}$$

where p and M are the proton momentum and mass. The expression (5) is valid if $X_0 < X < X_1$, which takes place in our case. Thereby, for the value (4), multiplied by the target thickness, we get 311.6 keV. As expected, this value is slightly larger than the one presented in Fig. 5 by the dashed line (301.5 keV). Nevertheless, as we see, these quantities are rather close to each other. Their ratio amounts to 0.968 and approaches unity with the increase of E_0. For instance, at $E_0 = 2$ MeV, which is still much less than $E_{\rm max}$, this ratio is 0.997, which can be considered as undistinguishable from unity, taking into account a possible achievable precision of the experimental measurement of $E_{\rm AV}$.

Note that for protons with momentum $p = 15$ GeV/c the density effect in the ionization loss is not manifested to full extent as for higher p. Thus, it is natural to expect some change of the values of $E_{\rm MP}$ and $E_{\rm AV}$ with the increase of p until they reach the Fermi plateau and cease to depend on p. Though, this change is rather small, since already at 15 GeV/c these values are rather close to their asymptotic values at the plateau. For instance, the value of $E_{\rm MP}$ for a sufficiently high-energy proton in a disoriented 900 μm silicon target is 275 keV, while at 15 GeV/c it is 263 keV (see Fig. 4). This presumes that at higher p the ILS in a disoriented crystal is rather close to the one presented in Fig. 2. The same concerns the spectrum in the oriented crystal in this figure, with the only addition that the hump due to above-barrier particles will decrease with the increase of the proton energy (provided the target thickness is fixed), which is caused by the increase of the dechanneling length. Hence, at higher proton energies it is natural to expect the dependences $E_{\rm MP}(\theta)$ and $E_{\rm AV}(\theta)$ which are rather close to the ones presented in Figs. 4 and 5, taking into account that the typical parameter θ_c of these dependences scales as $p^{-1/2}$.

4 Conclusions

The paper presents the first results of investigation of orientational dependence of high-energy particle ionization loss spectrum (ILS) in silicon crystals. The evolution of 15 GeV/c proton ILS with the change of the angle θ between the particle momentum and the crystal plane (110) is considered on the basis of computer simulation. It is shown that in this case the shape of the spectrum noticeably changes, being considerably different from the Landau distribution in the intermediate range of θ separating the planar channeling mode of the particle motion and the above-barrier mode typical for disoriented crystals. The behavior of the most probable energy loss and the average restricted energy loss is considered. It is demonstrated that both these quantities change nonmonotonically with the increase of θ, reaching some maximum values at $\theta \approx \theta_c$ which are larger than the corresponding values of these quantities in disoriented crystals. Such an increase of the loss of positively charged particles compared to their loss in a disoriented crystal is associated with the 'hanging' mode

[3] It is assumed that $E_1 \ll E_{\rm max}$, where $E_{\rm max}$ is the kinematic maximum energy which can be transferred by the proton to an atomic electron in a single collision.

of motion. In this mode the particles slow down (in the transverse direction) in the vicinity of crystal planes and spend relatively large periods of time in the region of huge atomic electron density. Moreover, the dependence of E_{MP} on θ in the considered case is not only non-monotonic, but also discontinuous. Additionally, the influence of dechanneling and the impact of the incident beam divergence angle of one θ_c on ILS of planar channeled protons are demonstrated. Generally, the presented results show that ILS of high-energy particles in oriented crystals are rather sensitive to peculiarities of the particle motion and, in principle, could be applied for experimental investigation of these peculiarities. The obtained results may be also important for the correct interpretation of the signal received from semiconductor particle detectors in the case when one of their crystallographic planes accidentally happens to be almost parallel to the incident particle velocity. Let us finally note that in [31] a significant dependence of the probability of close collisions on the angle between the crystal *axis* and the direction of the incident particle momentum has been demonstrated. Further it is planned to investigate the manifestation of this dependence in the particle ILS.

Acknowledgements The work was partially supported by the project No. 0124U002155 of the National Academy of Sciences of Ukraine. S.V. Trofymenko acknowledges support from the National Academy of Sciences of Ukraine, Grant no. 0124U003625. I.V. Kyryllin acknowledges support from the National Research Foundation of Ukraine, Grant no. 0123U105211 (222/0004).

Data Availability Statement My manuscript has no associated data. [Authors' comment: All the data generated or analysed during this study are included into the article.]

Code Availability Statement My manuscript has no associated code /software. [Authors' comment: No code/software was analysed during the current study.]

Funded by SCOAP[3].

References

1. L.D. Landau, J. Phys. USSR **8**, 201 (1944)
2. P.V. Vavilov, Sov. Phys. JETP **5**, 749 (1957). [Zh. Exp. Teor. Fiz. 32, 920 (1957)]
3. O. Blunck, S. Leisegang, Z. Physik **128**, 500 (1950)
4. P. Shulek, B.M. Golovin, L.A. Kuliukina et al., Sov. J. Nucl. Phys. **4**, 400 (1967). [Yad. Fiz. 4, 564 (1967)]
5. R. Talman, Nucl. Instrum. Methods **159**, 189 (1979)
6. H. Bichsel, Rev. Mod. Phys. **60**, 663 (1988)
7. W.W.M. Allison, J.H. Cobb, Annu. Rev. Nucl. Part. Sci. **30**, 253 (1980)
8. J.F. Bak, A. Burenkov, J.B.B. Petersen et al., Nucl. Phys. B **288**, 681 (1987)
9. S. Meroli, D. Passeri, L. Servoli, J. Inst. **6**, P06013 (2011)
10. A.V. Shchagin, N.F. Shul'ga, S.V. Trofymenko et al., Nucl. Instrum. Methods B **387**, 29 (2016)
11. R.M. Nazhmudinov, A.S. Kubankin, A.V. Shchagin et al., Nucl. Instrum. Methods B **391**, 69 (2017)
12. T. Virkus, H.D. Thomsen, E. Uggerhøj, U.I. Uggerhøj, S. Ballestrero et al., Phys. Rev. Lett. **100**, 164802 (2008)
13. H.D. Thomsen, U.I. Uggerhøj, Nucl. Instrum. Methods Phys. Res. Sect. B **269**, 1919 (2011)
14. S.V. Trofymenko, Eur. Phys. J. C **83**, 32 (2023)
15. O.B. Kolcu, Ordu Univ. J. Sci. Technol. **13**, 154 (2023)
16. O. Fich, J.A. Golovchenko, K.O. Nielsen et al., Phys. Rev. Lett. **36**, 1245 (1976)
17. H. Esbensen, O. Fich, J.A. Golovchenko et al., Nucl. Phys. B **127**, 281 (1977)
18. H. Esbensen, O. Fich, J.A. Golovchenko et al., Phys. Rev. B **18**, 1039 (1978)
19. S. Pape Møller, V. Biryukov, S. Datz et al., Phys. Rev. A **64**, 032902 (2001)
20. J. Lindhard, Danske Vid. Selsk. Mat. Fys. Medd. **34**, 14 (1965)
21. S.V. Trofymenko, I.V. Kyryllin, Eur. Phys. J. C **80**, 689 (2020)
22. A.V. Shchagin, G. Kube, S.A. Strokov, W. Lauth, Nucl. Instrum. Methods A **1059**, 168930 (2024)
23. S.V. Trofymenko, N.F. Shul'ga, Phys. Rev. Accel. Beams **23**, 084501 (2020)
24. N.F. Shul'ga, I.V. Kirillin, V.I. Truten', J. Surf. Invest. X-Ray Synchrotron Neutron Tech. **7**, 398 (2013)
25. I.V. Kirillin, N.F. Shul'ga, L. Bandiera et al., Eur. Phys. J. C **77**, 117 (2017)
26. I.V. Kirillin, Phys. Rev. Accel. Beams **20**, 104401 (2017)
27. I.V. Kyryllin, N.F. Shul'ga, Eur. Phys. J. C **79**, 1015 (2019)
28. I.V. Kirillin, N.F. Shul'ga, Nucl. Instrum. Methods B **402**, 40 (2017)
29. M. Tanabashi, K. Hagiwara, K. Hikasa et al. (Particle Data Group), Phys. Rev. D **98**, 030001 (2018)
30. R.M. Sternheimer, R.F. Peierls, Phys. Rev. B **3**, 3681 (1971)
31. Yu.A. Chesnokov, I.V. Kirillin, W. Scandale et al., Phys. Lett. B **731**, 118 (2014)